

# First Seconds in a Building's Life—In Situ Synchrotron X-Ray Diffraction Study of Cement Hydration on the Millisecond Timescale\*\*

Moritz-Caspar Schlegel, Adnan Sarfraz, Urs Müller, Ulrich Panne, and Franziska Emmerling\*

Upon the initial contact of cement with water, the resulting system represents a colloidal suspension consisting of reacting crystalline and amorphous phases. Ordinary portland cement (OPC) is a complex multiphase system made up of several crystalline phases. These phases are stable at ambient conditions in up to seven different modifications, which are stabilized by various alkali-metal ions, or they exist as a solid solution.<sup>[1]</sup> During hydration, the formation of the structurally more complex hydration products leads to the setting of the cement and subsequently to the hardening of the cement paste. Detailed insight into the different stages of the hydration processes is essential for a more complete understanding of how these processes can be effectively influenced. In particular, the phase development at the beginning of hydration is not yet well understood.<sup>[2]</sup> This fact can be ascribed to the limitations of the analytical methods used to study the highly dynamic phase development. One of these highly dynamic processes is the initial reaction of the cement component C<sub>3</sub>A (Ca<sub>3</sub>Al<sub>2</sub>O<sub>6</sub>) with SO<sub>4</sub><sup>2-</sup> ions to form ettringite (Ca<sub>6</sub>Al<sub>2</sub>(SO<sub>4</sub>)<sub>3</sub>(OH)<sub>12</sub>·26H<sub>2</sub>O).<sup>[3]</sup>

Nowadays, the hydration processes at early stages are more often influenced by organic additives such as retarding admixtures and superplasticizers.<sup>[4–6]</sup> These additives are used to optimize the flow properties of the cement paste during construction and reduce the water/cement ratio providing higher compressive strength.<sup>[7]</sup> The organic additives are most influential during the first minutes of the hydration.<sup>[8]</sup> The formation of the initial hydrate phases is affected and the resulting microstructure and phase composition are different from that of cement without additives.<sup>[9–11]</sup> Polycarboxylate ethers (PCEs) are commonly used superplasticizers because of their strong dispersion effect.<sup>[12]</sup>

The focus of previous studies was usually on the change of the rheological behavior of the cement paste and the key factors of the PCE adsorption process.<sup>[13–18]</sup> The formation of the hydrate phases is often interpreted based on the change of fluid behaviors and zeta potentials, but not characterized by analyzing the crystallization processes directly.<sup>[3,19,20]</sup>

Up to now, the very first stages of the crystallization process of cement have never been characterized in detail.

Furthermore there is no analytical evidence for the influence of PCEs on this initial crystallization.<sup>[20]</sup> Therefore, the objective of our study was the in situ analysis of the initial hydration processes. We utilized high-resolution synchrotron X-ray diffraction (SyXRD) to analyze the early formation of ettringite and the interaction of PCE with cement particle surfaces. For comparison, PCEs with different polymer charge density were selected.

The origin of the dispersion effect associated with PCE is frequently discussed in literature.<sup>[5,12,19]</sup> Their effect is mainly described based on charge and adsorption effects during the cement hydration. Zeta potential measurements indicate that the PCE polymer backbone adsorbs primarily at the surface of hydrates from the cement phase C<sub>3</sub>A. The surface of C<sub>3</sub>A is positively charged, whereas the cement's silicate phases, C<sub>3</sub>S and C<sub>2</sub>S, have negative zeta potentials. After adsorption, the side chains of the polymer are orientated away from the phase surface and extend into the pores.<sup>[21]</sup> Finally, steric repulsion between the cement particles of the cement paste leads to stabilization of the suspension (Figure 1).<sup>[22,23]</sup> The reaction of C<sub>3</sub>A with SO<sub>4</sub><sup>2-</sup> ions in the pore solution to give ettringite is thus retarded and decreased. After the initial adsorption, the PCE is subsequently replaced by SO<sub>4</sub><sup>2-</sup> ions. The time and intensity of the PCE–particle interaction depends on the PCE modification and the charge density of the polymer backbone. The hydration process for pure OPC and OPC mixed with different PCE additives was followed in situ (Figure 2 and Figures S1–S4 in the Supporting Information). The initial ettringite reflections are observed for all four specimens. The formation of ettringite is coupled with the PCE adsorption, and analyzing this formation stage offers additional informa-

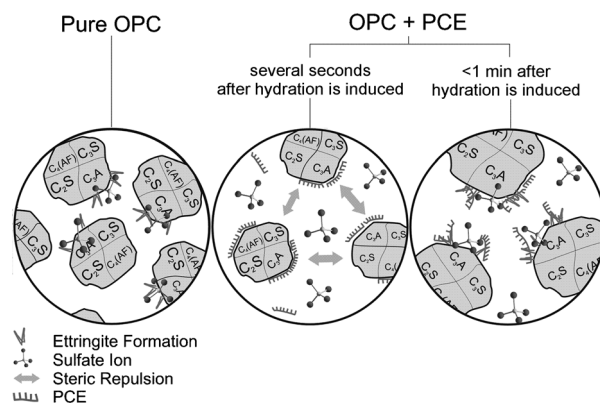


**Figure 1.** After the start of hydration, C<sub>3</sub>A reacts immediately with sulfate ions to form ettringite (left). PCE adsorbs primarily at the C<sub>3</sub>A surface. The suspension is stabilized by steric repulsion (middle). After the initial adsorption, sulfate ions replace the PCE (right).

[\*] M.-C. Schlegel, A. Sarfraz, U. Müller, U. Panne, Dr. F. Emmerling  
 BAM Federal Institute of Materials Research and Testing  
 Richard-Willstätter-Strasse 11, 12489 Berlin (Germany)  
 E-mail: franziska.emmerling@bam.de

[\*\*] We thank the ESRF, Grenoble, France for support. M.C.S. thanks the BAM Federal Institute for Materials Research and Testing, Berlin (Germany) for a PhD stipend.

Supporting information for this article is available on the WWW under <http://dx.doi.org/10.1002/anie.201200993>.

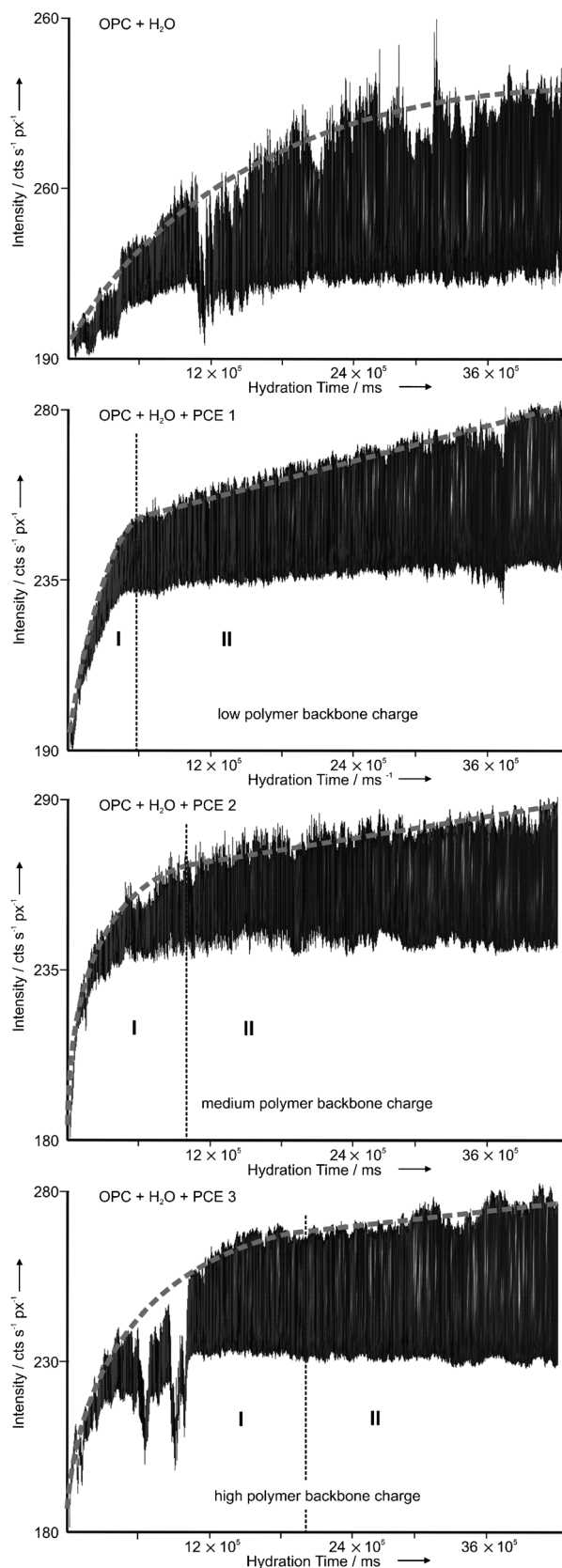


**Figure 2.** Plot of ettringite (100) reflections as a function of time. The growth process can be separated into an initial exponential (I) and a linear (II) increase of the reflection intensity (dashed line). The higher the charge density of the PCE, the greater the delay in the initial ettringite formation and the later the onset of the linear increase of the reflection intensity.  $\text{cts s}^{-1} \text{px}^{-1}$  = counts per second and pixel.

tion about the early hydration processes and the effect of the PCE.

In Figure 2, the ettringite (100) reflections are plotted as a function of time. The full-width at half-maximum (FWHM) of this reflection does not change significantly during the hydration. Thus, the peak intensity is an indicator of the amount of initially formed ettringite. Observing this reflection gives an overview about how the ettringite formation changes as a result of PCE adsorption. Owing to the irregular shape of the specimen, the sample position fluctuates at the beginning of the experiment. This effect leads to stronger variations of the reflections intensities during the first two minutes of the hydration of OPC and of OPC with PCE 3. Since a clear trend in the reflection intensities is evident, this sample effect is not included in the interpretation of the initial cement hydration.

During the first minutes of hydration, the intensity increase of the PCE-containing OPCs differs from that of pure OPC. All measurement series display an increase in the background contribution during the water injection. This leads to an increase of the intensities over the first part of the  $q$  range. However, the increase of the background is more pronounced for the PCE-containing specimens.

The ettringite (100) reflection of the pure OPC displays an exponential increase over the whole time span of hydration. The increase of the PCE-containing OPC is much quicker and can be separated into an initial exponential (I) and a linear (II) increase of the reflection intensity (see labels in Figure 2). The higher the PCE backbone charge density, the later the onset of the linear increase occurs.

The different hydration behavior of the specimen is driven by the anionic charge densities of the PCE. The  $\text{C}_3\text{A}$  in pure OPC is converted into ettringite as a function of the residual sulfate in the pore solution. This hydration behavior results in a high initial formation of ettringite and its amount increases as a function of time. The ettringite formation in PCE-containing OPC is additionally influenced by the backbone charge density of the respective PCE.

At the beginning of the hydration, PCE adsorbs at the  $\text{C}_3\text{A}$  surface rapidly and only a small amount of ettringite crystallizes. During the adsorption, the PCE is replaced by sulfate ions of the pore solution. An equilibrium results between PCE adsorption and its replacement by  $\text{SO}_4^{2-}$  ions, which leads to a linear increase of the ettringite amount. Consequently, a higher polymer backbone charge leads to a retarded adjustment of the equilibration state. Thus fewer sulfate ions replace PCE and the inhibition of ettringite formation is decelerated. The observed increasing background signal results from the increased amount of free water remaining in the specimen, dissolution of crystalline phases, and the formation of X-ray amorphous phases.

Utilizing high-resolution SyXRD with a time resolution in the millisecond range, it is feasible to analyze the early crystallization processes of cement directly. The acoustic levitation system provides contact-free analysis without any influence of the container wall material on the crystallization process. This X-ray diffraction method provides a detailed characterization of the effect of the PCE on the initial ettringite formation. Evidently, the origin of the PCE

dispersion effect is a combination of 1) steric repulsion effect of the charged surfaces, 2) the higher amount of free water in the phase system as a result of the reduced formation of hydrate phases, and 3) the retarded formation of ettringite.

### Experimental Section

OPC pellets (Table S5 in the Supporting Information) were prepared with a molding press (15 s at 1 kbar). The pellets were cut into pieces each weighing 0.1 g. For contact-free analysis, the pellets were positioned in an acoustic levitator system (Figure 3) operating with a frequency of 58 kHz and a sound pressure level of 160 dB.<sup>[24–26]</sup> This kind of sample holder avoids any influence of the container wall

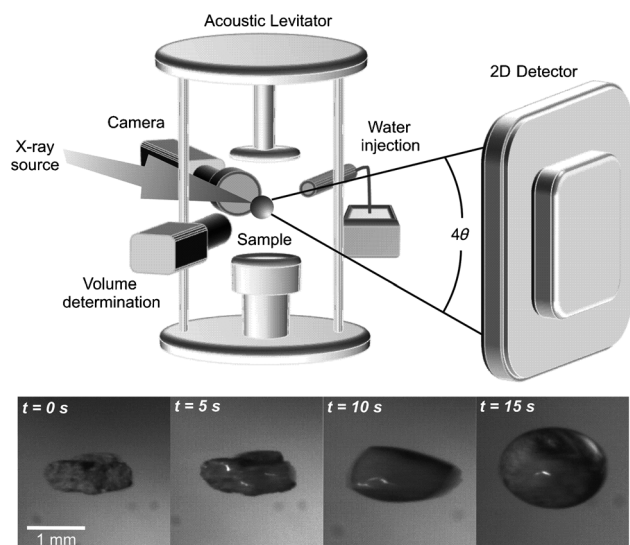


**Figure 3.** The experimental setup is suitable for contact-free analysis; hydration can be induced during the experiment.

material on the crystallization process. Three different PCE modifications with low (PCE 1, GLENIUM SKY 591 (FM), BASF, Gloethe, Germany), medium (PCE 2, GLENIUM SKY 593, BASF, Gloethe, Germany), and high polymer backbone charge density (PCE 3, GLENIUM SKY 595, BASF, Gloethe, Germany) were dissolved in distilled water and the solution was homogenized. The PCE amount was 2 wt% of the amount of OPC. In the course of the experiment, the solution was injected by a piezo-electric microdrop dispenser until a water/cement weight ratio of 0.50 was reached. The amount of the injected solution was controlled by monitoring the volume increase. The time-resolved in situ X-ray diffraction analysis was performed at the beamline ID11 at the synchrotron facility ESRF (European Synchrotron Research Facility). A wavelength of  $\lambda = 0.03444$  nm and a beam diameter of 100  $\mu\text{m}$  was chosen. In a typical experiment, the diffracted intensities were collected by a Frelon2K CCD detector located 110 mm behind the specimen. The data acquisition time of a single diffraction pattern was 500 ms, which provides high-resolution time-resolved analysis. The measurements were carried out until a total hydration time of 7 min was reached. The detector images were processed and converted into diagrams of scattered intensities versus scattering vector  $q$  ( $q = 4\pi/\lambda \sin\theta$ ) employing an algorithm from the FIT2D software.<sup>[27]</sup> The phase identification was carried out by applying a search/match routine (EVA, BRUKER, Wiesbaden, Germany). Afterwards, the collected diffraction patterns were displayed in a side view were plotted versus time without background

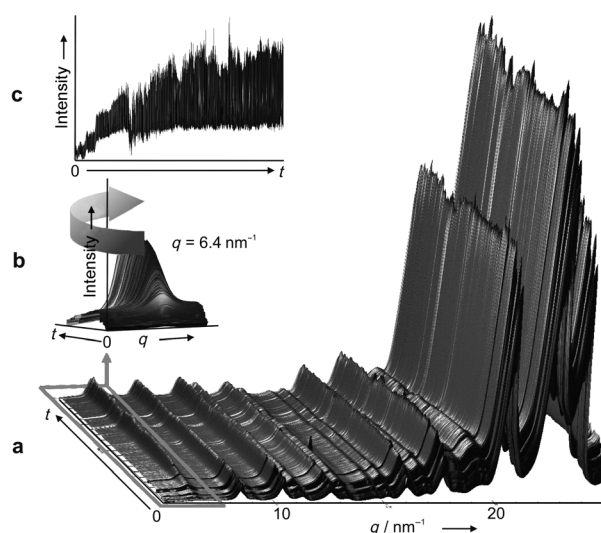


**Figure 4.** Diffraction pattern collected during the hydration of pure OPC (a). The ettringite (100) reflection is enlarged (b) and displayed in a stacked plot as a function of time (c).

correction. This provides a quick overview about both the development of the reflection and background intensities (Figure 4).

Received: February 6, 2012

Published online: April 11, 2012

**Keywords:** cement hydration · colloidal suspensions · in situ analysis · X-ray diffraction

- [1] H. F. W. Taylor, *Cement Chemistry*, 2nd ed., CPI Bath, London, **1997**.
- [2] A. N. Christensen, N. V. Y. Scarlett, I. C. Madsen, T. R. Jensen, J. C. Hanson, *Dalton Trans.* **2003**, 1529.
- [3] A. P. Kirchheim, D. C. Dal Molin, P. Fischer, A. H. Emwas, J. L. Provis, P. J. M. Monteiro, *Inorg. Chem.* **2011**, *50*, 1203.
- [4] J. Y. Petit, E. Wirquin, B. Duthoit, *Cem. Concr. Res.* **2005**, *35*, 256.
- [5] J. Plank, C. Schroeﬂ, M. Gruber, M. Lesti, R. Sieber, *J. Adv. Concr. Technol.* **2009**, *7*, 5.
- [6] R. J. Flatt, I. Schober, E. Raphael, C. Plassard, E. Lesniewska, *Langmuir* **2009**, *25*, 845.
- [7] K. Yamada, S. Ogawa, S. Hanehara, *Cem. Concr. Res.* **2001**, *31*, 375.
- [8] C. Jolicoeur, M. A. Simard, *Cem. Concr. Compos.* **1998**, *20*, 87.
- [9] M. Bishop, S. G. Bott, A. R. Barron, *Chem. Mater.* **2003**, *15*, 3074.
- [10] A. A. Bonapasta, F. Buda, P. Colombet, G. Guerrini, *Chem. Mater.* **2002**, *14*, 1016.
- [11] F. Ridi, L. Dei, E. Fratini, S. H. Chen, P. Baglioni, *J. Phys. Chem. B* **2003**, *107*, 1056.
- [12] M. Lesti, S. Ng, J. Plank, *J. Am. Ceram. Soc.* **2010**, *93*, 3493.
- [13] L. Ferrari, J. Kaufmann, F. Winnefeld, J. Plank, *J. Colloid Interface Sci.* **2010**, *347*, 15.
- [14] M. Gretz, J. Plank, *Colloids Surf. A* **2010**, *366*, 38.
- [15] J. Plank, C. Hirsch, *Cem. Concr. Res.* **2007**, *37*, 537.
- [16] J. Plank, K. Pollmann, N. Zouaoui, P. R. Andres, C. Schaefer, *Cem. Concr. Res.* **2008**, *38*, 1210.
- [17] J. Plank, B. Sachsenhauser, *Cem. Concr. Res.* **2009**, *39*, 1.
- [18] J. Plank, B. Sachsenhauser, J. de Reese, *Cem. Concr. Res.* **2010**, *40*, 699.

- [19] C. Giraudeau, J. B. D. de Lacaillerie, Z. Souguir, A. Nonat, R. J. Flatt, *J. Am. Ceram. Soc.* **2009**, *92*, 2471.
- [20] J. Plank, D. Zhimin, H. Keller, F. Von Hossle, W. Seidl, *Cem. Concr. Res.* **2010**, *40*, 45.
- [21] K. Yoshioka, E. Tazawa, K. Kawai, T. Enohata, *Cem. Concr. Res.* **2002**, *32*, 1507.
- [22] K. Yoshioka, E. Sakai, M. Daimon, A. Kitahara, *J. Am. Ceram. Soc.* **1997**, *80*, 2667.
- [23] H. Uchikawa, S. Hanehara, D. Sawaki, *Cem. Concr. Res.* **1997**, *27*, 37.
- [24] S. E. Wolf, J. Leiterer, M. Kappl, F. Emmerling, W. Tremel, *J. Am. Chem. Soc.* **2008**, *130*, 12342.
- [25] A. Sarfraz, M. C. Schlegel, J. Wright, F. Emmerling, *Chem. Commun.* **2011**, *47*, 9369.
- [26] J. Leiterer, W. Leitenberger, F. Emmerling, A. F. Thunemann, U. Panne, *J. Appl. Crystallogr.* **2006**, *39*, 771.
- [27] A. P. Hammersley, K. Brown, W. Burmeister, L. Claustre, A. Gonzalez, S. McSweeney, E. Mitchell, J. P. Moy, S. O. Svensson, A. W. Thompson, *J. Synchrotron Radiat.* **1997**, *4*, 67.
-